# Modeling Multiple Dam Breaks: A Case Study on the Hypothetical Failure of Adhaim and Makhool Dams

**Ahmed S. Al-Fahal**
Environmental Engineering Department, College of Engineering, Tikrit University, Tikrit, Iraq
ahmed.s.mahmood@tu.edu.iq (corresponding author)

**Rasul M. Khalaf**
Civil Engineering Department, College of Engineering, Mustansiriyah University, Bagdad, Iraq
rasulcon@uomstaniriyah.edu.iq

**Raad H. Irzooki**
Environmental Engineering Department, College of Engineering, Tikrit University, Tikrit, Iraq
dr.raadhoobi@tu.edu.iq

*Received: 21 April 2025 | Revised: 18 May 2025 and 4 June 2025 | Accepted: 6 June 2025*

 *DOI: https://doi.org/10.48084/etasr.11620*

## ABSTRACT

**This study examines the hypothetical consequences of the simultaneous failure of the Adhaim and Makhool dams in Iraq, focusing on the hydrological and socio-economic impacts. Advanced hydrodynamic modeling is used to simulate flood behavior, including the extent of inundation, the flood wave movement, and the timing of peak discharges downstream. The analysis considers the dam structural features, breach sizes, and downstream terrain. Simulation results indicate that serious consequences are likely, with heavy flooding posing a threat to urban areas, farmland, and critical infrastructure. These findings emphasize the urgent need for comprehensive risk assessments, effective emergency planning, and strategic mitigation efforts. The study provides insights for enhancing the dam safety and disaster resilience in hydraulically interconnected regions. It identifies critical zones of inundation, maximum flood depths, arrival times, and flood durations along the river corridor and across the floodplain. These findings highlight the greater hazard posed by the cascading dam failures compared to a single dam break. Additionally, the analysis underscores the importance of early warning systems and emergency preparedness. The outcomes provide valuable guidance for risk assessment, mitigation planning, and decision-making related to the dam safety and disaster management in the region.**

***Keywords-HEC-Ras model; dam break modeling; Adhaim dam; Makhool dam; flood hazard***

## I. INTRODUCTION

Dams are hydraulic structures constructed on rivers to form reservoirs that store water for multiple purposes, such as flood control, hydropower, urban and industrial water supply, irrigation, environmental preservation, improving low flows, and recreation [1]. Sudden dam failures cause huge destruction in the region, particularly affecting the downstream communities. They cause property and loss of lives, environmental pollution along the inundation path, and alter the river morphology through erosion and sediment deposition. Multiple dam failures can have severe consequences as the cumulative flow increases. The increased risk of dam failure raises safety concerns, particularly when dam sites are located near a large river downstream from a substantial catchment area. Therefore, managing the floods caused by extreme hydrological events, especially after multiple dam failures, is very important [2]. Since individual dam breach parameters can significantly influence the simulation of dam-induced floods, a reasonable set of parameters is typically used across multiple dam breach scenarios. On the night of September 10, 2023, two dams in Libya catastrophically failed, causing a large part of Derna city, located downstream, to be destroyed by water and debris. Over 6,000 people died in the flood, and thousands more were forced to leave the city. The heavy rainfall caused by Daniel's Medicine led to intense precipitation and the overflowing of the dams once they reached capacity, ultimately leading to their failure. Flooding caused by dam failure and other flows can result in significant property damage, as well as fatalities [3].

Dams offer significant benefits to society, but they also pose risks of failure that can lead to serious consequences. Dam failure can be generated by several factors, including

overtopping caused by inadequate spillway design or insufficient reservoir capacity for large inflows [4]. Piping can also cause failure if seepage carries away fine materials along the upstream-downstream path, and settlements may occur due to landslides on the dam's sides. Earthquakes and foundation failure can further contribute to dam liquefaction [5]. Additionally, changes in the amount of discharge can modify the flow energy in waterways, which might impact the hydraulic conditions downstream and potentially lead to structural stress or instability under certain circumstances. About one-third of dam failures are caused by overtopping [6].

Although dam collapses are extremely rare, they can cause extensive damage and even fatalities when they happen. When constructing and operating dams, safety must be a top priority, as numerous dams worldwide have failed in the past, resulting in severe damage to property, loss of life, and ecological harm. To minimize the risk of failure, it is essential to address the hazards associated with the water storage consistently. Both dam owners and design engineers share responsibility for the potentially catastrophic consequences of dam failures [7].

Every dam has a risk of failure that could result in catastrophic downstream flooding. These failures are hazardous because they involve the sudden release of large water volumes at high flow rates within a short time, making them more likely than routine floods to cause structural damage and loss of life. For instance, the 1976 failure of the Teton Dam in the United States, a 93-m-tall rocky fill dam, was caused by piping just before the reservoir was fully filled. This disaster led to ten deaths, injuries to two thousand people, and damage to over seven thousand homes [8]. Similarly, in 1982, a severe storm in Spain caused the collapse of the Tous rockfill dam, resulting in flooding over 300 km² of cities and affected regions, and injuring approximately 200,000 people [9]. According to [10], there have been over 350 dam failures in the United States from January 2000 to November 2022. Developing a comprehensive plan for the dam failure response and implementing proactive measures to minimize the impact of potential catastrophic events are crucial, especially considering the climate change and its role in increasing extreme precipitation events [11].

Dam failures are often caused by hydrological events influenced by climate change, earthquakes, and improper spillway management. Various dam types have failed due to such events, but most failures have involved earthen dams, often triggered by flooding. Earth dams are less rigid and thus more prone to failure. Earthen dams, like other engineering structures, can collapse due to poor design, faulty construction, lack of maintenance, and other factors. The various causes of earth dam failures can be grouped into three main types: hydraulic, seepage, and structural failures. Hydraulic failures account for about 40% of all cases and typically occur due to overtopping, erosion of the upstream or downstream surfaces, and cracking caused by hydraulic forces. Seepage-related failures account for roughly 35% of the incidents, and are primarily caused by piping through the foundation or dam body, as well as sloughing at the downstream toe. Structural failures, which account for approximately 25% of the earth dam failures, typically involve the sliding of the foundation or embankment [12]. Understanding the relative frequency and mechanisms of these failure types is essential for effective dam design, maintenance, and risk mitigation [12], as shown in Table I.

TABLE I. CLASSIFICATION OF THE TYPES OF DAM FAILURE.

| # | Status | Percentage % |
|---|---|---|
| 1 | Hydraulic failure | 40 |
| 2 | Seepage failure | 35 |
| 3 | Structural failure | 25 |

Dam failures, often caused by reservoir overtopping or structural breaches, can result in catastrophic flooding, extensive property damage, and significant loss of life. Recent failures have underscored the crucial importance of advanced dam break modeling in evaluating hazards, guiding risk mitigation efforts, and supporting emergency planning. The accurate simulation of the dam breach processes is crucial for ensuring operational safety, maintaining infrastructure, and enhancing disaster readiness [13]. Authors in [14] examined the Brumadinho dam failure in Brazil, which resulted in more than 248 deaths and approximately $2.88 billion in damages. Using the Hydrologic Engineering Center's River Analysis System (HEC-RAS) along with NASA's Shuttle Radar Topography Mission (SRTM), the elevation data modeled the sediment flow and flood spread, generating results consistent with actual inundation patterns. Their findings endorse the application of these models for predicting future dam break events. In [15], the behavior of a dam-break wave composed of a clay-water mixture under turbulent flow conditions and its interaction with a vertical wall were analyzed. Researchers used three-dimensional large eddy simulations, combining the dynamic Smagorinsky model with the volume-of-fluid method, to monitor the wave's development over time. A power-law model represented the non-Newtonian properties of the mixture. The results showed that the bed shear stresses in non-Newtonian simulations were approximately twice those in clear water, while the peak impact force decreased slightly as the clay concentration increased. Larger-scale tests indicated increased wave speeds and shear stresses, but the peak impact force remained consistent across different scales. These findings demonstrate that small-scale tests can reliably predict critical forces relevant to engineering design. Authors in [16] employed HEC-RAS to simulate the Temenggor Dam failure under scenarios involving piping and overtopping. The 1D model forecasted peak flows of 281,588 m³/s (piping) and 331,030 m³/s (overtopping), whereas the 2D model estimated 268,341 m³/s and 328,869 m³/s, respectively. The arrival times of flood waves were also determined. While the 1D model required less computational time, the 2D model provided a more detailed inundation map, which aided in hazard assessment and emergency response planning.

HEC-RAS 2D was used to model the dam-break wave propagation in an alpine valley, simulating a hypothetical failure of the Cancano I dam [17]. The results are closely aligned with TELEMAC 2D data and historical records, confirming the suitability of HEC-RAS for steep, mountainous terrains. HEC-RAS and flood modeling tools were used to analyze the Pulichintala Dam breach in Andhra Pradesh, India

[18]. The input data encompassed cross-sections, dam geometry, hydrographs, and rating curves. The model predicted discharges of 121,368.9 m³/s at the dam site and 84,042.91 m³/s downstream of the dam. Additionally, a sensitivity analysis assessed how Manning's roughness, the PMF, breach duration, and width influenced the flood behavior. In [19], a numerical study was conducted on the Wai Abu Dam to support the development of an Emergency Action Plan (EAP). The model demonstrated a peak outflow reduction of 7.36% (Q10) and 2.14% (QPMF), with minimal impact on downstream conditions. Six sub-districts were affected, experiencing flood depths of 1–2.5 m (Q10) and 2.9–4.2 m (QPMF). Authors in [20] employed HEC-RAS 5.0.7 to simulate 2D dam failure at Sermo Dam, specifically examining the overtopping triggered by heavy rainfall. The peak inflow reached 1276.6 m³/s, causing flooding over 9,394 ha with a maximum depth of 17 m. Eight sub-districts were impacted, and the piping scenario caused the largest inundation, affecting 5,112 ha. The findings emphasized the importance of early warning systems and structural mitigation measures.

A 2D flood model for Tikrit City was developed using HEC-RAS, utilizing data from the Ministry of Water Resources (2019–2022) [21]. The study employed HEC-HMS and HEC-RAS to simulate dam breach scenarios, creating flood hydrographs, inundation maps, and estimates of the arrival times. Overtopping resulted in higher peak discharges (up to 14,821 m³/s) compared to piping failures. The risk classification by the National Disaster Management Agency guided both structural (e.g., emergency spillways) and non-structural (e.g., community preparedness) mitigation strategies, leading to an 8.4% reduction in the flood extent. Calibrated with a Manning's coefficient of 0.031 and validated against aerial imagery, the model demonstrated a significant increase in flooded areas with rising discharge. An 800 m³/s flow resulted in a 13.7% increase in flooding, while a 1500 m³/s flow led to a 90.7% increase. The study highlighted that the eastern banks of the Tigris River are more vulnerable due to their lower elevation.

The failure of the Hemren Dam in Diyala Governorate, Iraq, was simulated using HEC-RAS and a Digital Elevation Model (DEM)-based terrain modeling approach. The flood wave was propagated downstream to the confluence of the Diyala and Tigris rivers. The analysis identified high-risk zones based on water depth and velocity, providing a foundation for long-term flood risk management and mitigation planning [22]. Authors in [23] examined the progressive failure of Seyhan and Çatalan Dams near Adana, Turkey. It modeled the dam breach scenarios caused by exceeding hazard thresholds, rather than by structural failure, using HEC-RAS to simulate the flood spread and effects. The findings informed floodplain management and provided suggestions for reducing the hazards downstream. In northeastern Romania, five reservoirs (Cal Alb, Movileni, Tătărăşeni, Negreni, and Hăneşti) were evaluated using 2D HEC-RAS modeling to analyze the Başeu multi-reservoir system [24]. The Cal Alb dam breach scenario tested the system's flood attenuation capacity under different inflow and storage conditions. Severity maps were created for multiple recurrence intervals, highlighting the system's importance in regional flood risk reduction in the context of climate change.

HEC-RAS 2D, combined with GIS, was used to simulate the flood wave resulting from the Hemrem dam failure in Diyala Governorate, Iraq, to assess the downstream hydraulic impacts. It identified residential zones at risk and proposed an emergency response plan, highlighting the value of 2D hydrodynamic modeling in risk assessment and mitigation strategies [25]. Authors in [26] simulated the sudden, total collapse of the Mosul and Badush Dams, Northern Iraq to analyze the water redistribution between them. Two models were created: one to estimate the Mosul Dam reservoir level based on pre-collapse data, and another to predict the resulting water level in the Badush reservoir. For each failure scenario, the simulation used a step-by-step approach to determine the final water level in Badush, its storage volume, and the amount transferred from Mosul. The model proved highly adaptable, accurately predicting Badush's post-failure conditions based on Mosul's pre-collapse level. It performs reliably across all potential failure stages of Mosul Dam. The results show that Badush Dam, at 330.4 m a.s.l., can handle the maximum flood wave generated by a full failure of Mosul Dam at 333 m a.s.l. [26].

Authors in [27] introduced a probabilistic method for evaluating the overtopping breach risks in grass-covered earth-fill embankments. By employing a Monte Carlo dam breach model, the researchers simulated the initiation and development of breaches based on the duration of the flow. The results showed that overtopping might not greatly lower the reservoir levels and could lead to multiple breaches occurring sequentially. These findings highlight the critical role of the overtopping risk in dam safety assessments [27]. Another study analyzed the dam failure using HEC-RAS and various scenarios in Istanbul, Turkey [28]. A dam failure model was created to gather information for areas prone to flooding. Nine breach scenarios were analyzed in [29], revealing that while multi-reservoir systems can mitigate flooding, infrastructure deterioration resulting from climate change may lead to catastrophic failure. The study makes parallels to the Wadi Derna dam failures in Libya and introduces a modeling approach for assessing complex failure scenarios in future infrastructure design.

This study examines multi-dam failure scenarios, with a focus on the upper probable maximum discharge, arrival time, and peak flood height. It underscores the importance of accurately characterizing flood hydrographs, especially during extreme events, and distinguishes between flash floods and extreme floods by highlighting the greater demands on infrastructure safety assessments in the latter. Special attention is given to the runoff dynamics in multi-reservoir systems. The novelty of this study lies in modeling multiple dam failures, including hypothetical scenarios in different locations, which have not been studied before as a multi-failure case for these dams. The two-dimensional HEC-RAS numerical model simulates failure scenarios and finds potential failure points, generating two-dimensional maps that illustrate the flood inundation areas.

## II. METHODOLOGY

Dam failures can result from structural issues, extreme hydrological events, or human error, often leading to a sudden

release of the stored water and severe downstream consequences. Understanding the mechanisms, causes, and impacts of dam failures is crucial for mitigating the risks and enhancing the preparedness in vulnerable areas. The literature thoroughly documents past dam failures, providing insights into contributing factors and related social, economic, and environmental impacts. This study reviews existing research, highlights key issues and gaps, and proposes directions for future research [30]. Approximately 70% of the major dams in Iraq are built using naturally erodible materials, which makes them more vulnerable to failure. Therefore, detailed breach assessments are essential to reduce the flood risks related to dam failure. Embankment dams are usually made of materials, like earth, rock, clay, or other erosion-resistant substances. Among the various types, rock-fill and earth-fill dams are the most common [31]. Several empirical equations have been developed to estimate the dam breach parameters, such as breach width and time to failure, based on data from documented dam failures. Although these equations are primarily derived from small to medium-sized dams, they are applicable to a wide range of dam types and sizes. Notable models include those proposed in [32-37]. Among them, the equations in [32] are considered the most suitable for predicting the breach parameters in earthen dams. It was presented that the average side slopes are 1H:1V for bypass failure and 0.7 H:1V for pipe failure and leakage. These equations are:

$$B_{avg} = 0.27\, K_0\, {V_w}^{0.32}\ {H_b}^{0.04} \quad (1)$$

$$t_f = 63.2\ \left(\frac{V_w}{{H_b}^2}\right)^{0.5} \quad (2)$$

Hydrodynamic modeling is a crucial tool for predicting the flood flows and assessing their impact on infrastructure. Its success relies on solid theoretical principles, proper model selection, high-quality data, accurate calibration, and thorough quality assurance. When appropriately used, these models provide valuable insights into various water resource issues. However, misuse—arising from a lack of understanding of the model assumptions, data requirements, and limitations—can lead to overconfidence in the results and inefficient use of resources. While simplified models are appealing due to their ease, they often involve a trade-off between collecting extensive data and relying on assumptions that can obscure uncertainties [38]. Creating a hydrodynamic model involves selecting suitable governing equations, defining the spatial dimensions, and employing appropriate numerical methods. Typically, the two-dimensional Navier-Stokes equations are simplified to the Shallow Water Equations (SWE) or the Diffusion Wave Equations (DWE) for practical applications. The finite volume method is the most common numerical approach. In this study, the SWE, derived from the continuity and momentum equations, is used to simulate potential flood-prone areas using the finite volume method [39]:

$$\frac{\partial H}{\partial t} + \frac{\partial (p)}{\partial x} + \frac{\partial (q)}{\partial y} = 0 \quad (3)$$

$$\frac{\partial p}{\partial t} + \frac{\partial}{\partial x}\frac{p^2}{h} + \frac{\partial}{\partial y}\frac{(pq)}{h} = -\frac{n^2 p g\sqrt{p^2+q^2}}{h^2} - gh\frac{\partial H}{\partial x} + pf\frac{\partial}{p\partial x}(h\tau_{xx}) + \frac{\partial}{p\partial y}(h\tau_{xy}) \quad (4)$$

$$\frac{\partial q}{\partial t} + \frac{\partial}{\partial x}\frac{q^2}{h} + \frac{\partial}{\partial x}\frac{(pq)}{h} = -\frac{n^2 p g\sqrt{p^2+q^2}}{h^2} - gh\frac{\partial H}{\partial y} + pf\frac{\partial}{p\partial y}(h\tau_{yy}) + \frac{\partial}{p\partial x}(h\tau_{xy}) \quad (5)$$

The HEC-RAS modeling system, developed by the U.S. Army Corps of Engineers [39], provides a computational framework for simulating the river hydraulics using one-dimensional, two-dimensional, or combined numerical approaches. Recent updates have added two-dimensional modeling features, allowing the simulation of flow in narrow and wide prismatic channels, lakes, and floodplains. These simulations rely on hydrodynamic equations of motion in Cartesian coordinates, solved via a finite difference, stored-values implicit method. Both momentum and kinetic energy equations are handled implicitly. The model provides water surface elevations and velocity profiles across the channel and floodplain at each time step [40]. It also includes a sediment transport module that uses user-defined total load sediments or rating curves for bed load and suspended load transport.

The HEC-RAS model simulates the dam breach scenarios by routing inflows through the reservoir, estimating the breach characteristics, and modeling the downstream flow propagation. It uses empirical formulas, such as those in [32, 37], to determine the breach parameters. Hydrodynamic processes are represented via the SWE and DWE, which capture the rapid dynamics of the flood waves and flow velocities. The model depends on high-resolution terrain data to discretize the area into grid cells, reducing detail loss. The 2D HEC-RAS software creates a detailed table of hydraulic properties for each cell face, maintaining topography and supporting larger time steps. The simulation's time step is automatically adjusted based on the flow conditions and mesh size. Its ability to model both open-channel hydraulics and sediment transport, along with its user-friendly design, makes it a reliable tool for dam breach analysis [41]. Full momentum is calculated by:

$$C_r = \frac{V_w}{\left(\frac{\Delta_t}{\Delta_x}\right)} < 1.0 \quad (6)$$

The diffusion wave is calculated by:

$$C_r = \frac{V_w}{\left(\frac{\Delta_t}{\Delta_x}\right)} < 2.0 \quad (7)$$

The discretization process is the first step in numerical modeling, transforming the differential form of the SWE into algebraic equations that represent the computed variable at specific points in the time and space domains [42]. The finite volume method is a numerical approach used to solve partial differential equations that lack analytical solutions, such as the Saint-Venant equations. It involves dividing the computational domain into non-overlapping cells (regular or irregular) that collectively cover the entire area, facilitating the modeling of complex engineering problems. Once the mesh is set up, the governing equations are applied to each control volume. This method solves the Saint-Venant equations by calculating flow variables, such as depth and velocity, at each cell. The solution's accuracy depends on estimating the fluxes across the surfaces of all cells in the network [43]. Simulating dam break scenarios using 2D HEC-RAS requires collecting

comprehensive data, usually divided into geographic and hydraulic datasets. Geographic data include the DEM and Land Cover (LC) maps that define the area's physical features. Hydraulic data encompass flow parameters, such as the dam dimensions, the Probable Maximum Flood (PMF), and the reservoir volume. For sediment transport studies, extra inputs, such as sediment types and soil properties, are also needed. The model serves as a predictive tool for the flood spread, considering factors, such as the channel slope and flow resistance, which become increasingly significant as the flood wave advances. LC data help estimate Manning's roughness coefficient (n). The simulation involves two main sub-models: the dam breach model and the hydrodynamic model. The dam breach model determines the breach parameters and generates the failure hydrograph, which provides the upstream boundary condition for the hydrodynamic model. This second model forecasts downstream flood characteristics, including the water depth, velocity, surface elevation, and wave travel time. Sediment transport modeling evaluates the erosion patterns and identifies the potential sediment deposition zones downstream, as illustrated in Figure 1.

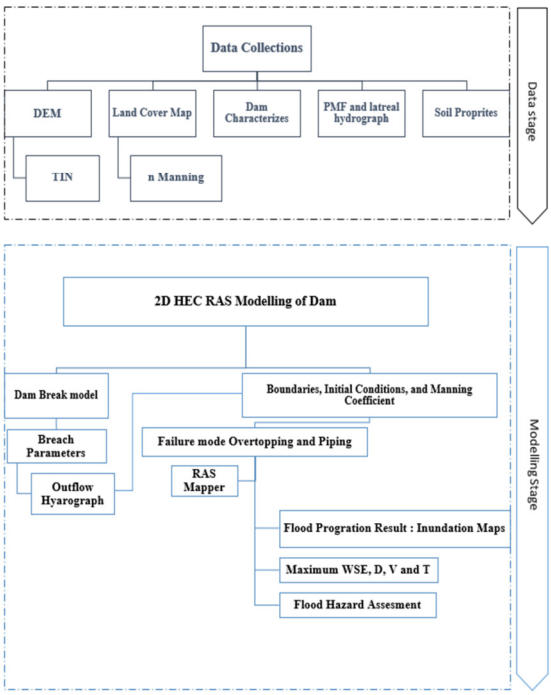


Fig. 1. Diagram of methodology.

The Tigris River, the largest in the Near East, begins in Turkey and mainly flows through Iraq. The Iraqi Tigris Basin extends along Iran's eastern border and includes the region's highest mountain ranges, which run parallel to the river. These mountains are the source of the Tigris' main left-bank tributaries: the Diyala, Greater Zab, and Lesser Zab rivers. The Adhaim River Basin is situated in the piedmont zone of the watershed. In contrast, the right bank consists mainly of semi-desert terrain with only ephemeral valleys that flow during the rainy season and lack significant tributaries. The Greater Zab joins the Tigris 50 km downstream of Mosul, draining an area of 26,470 km², while the Lesser Zab, with a catchment area of 22,250 km², joins the Tigris roughly 220 km north of Baghdad [44]. The Tigris River plays a vital role in Iraq's agriculture. The river shows significant flow changes, with recorded peaks at Mosul of 7,740 m³/s before the construction of the Mosul Dam and 302 m³/s afterward. The peak discharge usually happens in April–May, while the lowest flows occur in November–December. Figure 2 depicts the study area along the river stretch.

Adhaim Dam, an earth-fill structure within a designated zone in Diyala Governorate, Iraq, was constructed in 1999 for flood control, irrigation, and water supply purposes. The dam measures 3,800 m in length, 76.5 m in height, and has a crest elevation of 146.5 m. Its reservoir is entirely located in Iraq's northeastern region, between latitude 34.566036° N and longitude 44.513131° E [45]. Makhool Dam, currently under construction, is an earth-fill structure located on the Tigris River near Sharquat City. The Makhool reservoir is situated at approximately 35.1569° N latitude and 43.4316° E longitude [46].

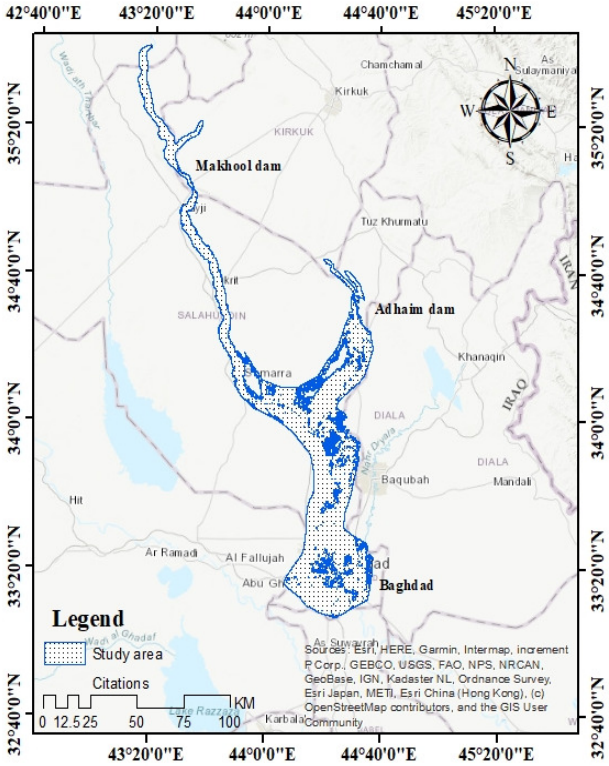


Fig. 2. Map of the reach study area.

Iraq's climate is mostly continental and semi-arid in the subtropical zone, except in the northern and northeastern mountainous regions, which have a Mediterranean climate. Winters tend to be cold, while summers are dry with high to extreme temperatures. To analyze precipitation patterns under these different climate conditions, daily precipitation data from

Integrated Multi-Satellite Retrievals (IMERG) and monthly average precipitation rates from the NASA application used [47] are examined. Rainfall is seasonal, mainly occurring from December to February across most of the country, and from November to April in the north and northeast. The climate is also influenced by dry, dusty south, and southeasterly winds (April–June, September–November), as well as by northern and northwesterly winds that cause significant surface heating [48].

## III. RESULTS

Flood events along the Tigris River and its tributaries frequently happen because the river channels have limited capacity to handle the high water flows. Peak discharges in the Tigris and its tributaries tend to occur at different times, typically in February–March, March–April, and April–May. At Fat'ha, the maximum flow typically occurs from February to April. The extent and duration of flooding in the Tigris are influenced by the timing and strength of flows from its major tributaries. As shown in Table II, the peak discharges in the Tigris and its tributaries vary by year and month. The 1969 flood at Fat'ha, for instance, was mainly caused by a peak flow from the Greater Zab River [49].

TABLE II. MAX-WATER DISCHARGES UNDER NATURAL CONDITION

| River | Site | Date of maximum discharges | Observed maximum Discharges (cumec) | Max. WSE (m) | Maximum design discharge (cumec) | |
|---|---|---|---|---|---|---|
| | | | | | 1% Probability | 0.1% Probability |
| Tigris | Mosul | 2/5/72 | 7740 | 220.2 | 9500 | 13000 |
| G-Zab | Eski-kalak | 2/4/69 | 9710 | ---- | 9640 | 15700 |
| L-Zab | Altun-Kubri | 25/3/54 | 3420 | ---- | 5870 | 9340 |
| Tigris | Fatha | 3/4/69 | 16380 | 119.15 | 19200 | 26500 |

The soil properties in the study area differ with depth and location. The Al-Adhaim Basin features alluvial sediments, including heavy silt in tributaries and carbonate, silicate, and rare rock pebbles. Clastic sediments (mainly gravel, sand, and silt) range from less than 1 m-5 m in thickness and are often used for construction [39]. South of Mosul, the soil profiles shift from stiff to moderately hard gypsum layers and dark sandy silt with gravel fragments between the surface and 20 m depth. Near Tikrit, soil varies from gravel and sand to silty sand, loose silt, and coarse silt within the same depth range. According to the FAO soil database, the HEC-RAS model classifies these soils as Hydrologic Soil Group D, reflecting low infiltration capacity [50]. The study area's terrain was derived from a publicly available DEM obtained via SRTM, with a spatial resolution of 12.5 by 12.5 m, referenced to WGS 1984, UTM Zone 38N [51]. The DEM was used to delineate the drainage networks and watershed boundaries, and to support the simulation of hydrological processes, such as surface runoff and sediment transport [52]. A topographic analysis of the DEM reveals that south of Makhool Dam, the terrain consists of elevated, mountainous areas on the right side, gradually transitioning into flat plains as they approach Baghdad. The terrain also flattens near the confluence of the Adhaim and Tigris Rivers in Al-Dhuluiyah. The elevation ranges from 200 m near Makhool reservoir to 26 m in Baghdad, and from 160 m near the Adhaim reservoir to 40 m at its confluence with the Tigris [53]. The region's digital elevation model is displayed in Figure 3.

Landsat 8 satellite imagery was used to analyze the LC in the Tigris River region. The images were geometrically corrected and classified with the maximum likelihood method. Using Iraq's national LC map from the Ministry of Water Resources Planning, the area was categorized into seven LC types. Pre- and post-classification comparisons were then performed [54]. The DEM was imported into the 2D HEC-RAS Mapper and converted to a Triangular Irregular Network (TIN) for unsteady 2D flow analysis. The TIN elevation was adjusted within RAS Mapper, and a soil type layer specific to the study area was generated. Reservoirs and 2D flow areas were delineated using Google Earth imagery, and a computational grid was assigned to the model [52], as illustrated in Figure 4.

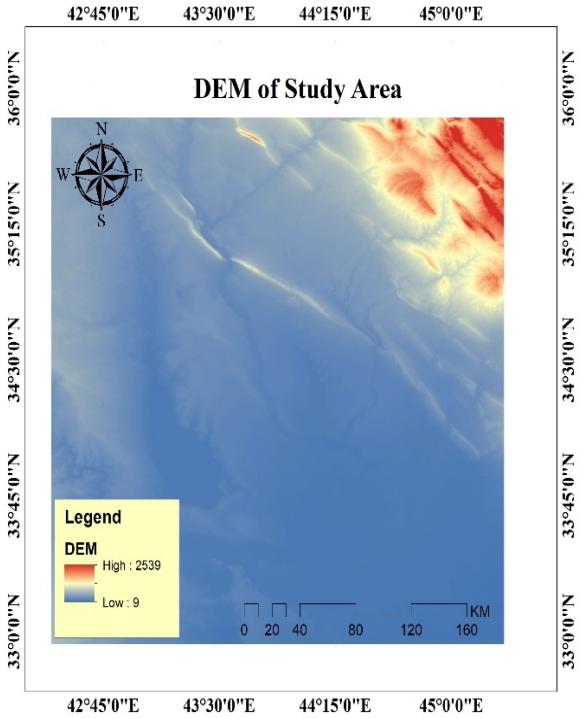


Fig. 3. DEM of the study area.

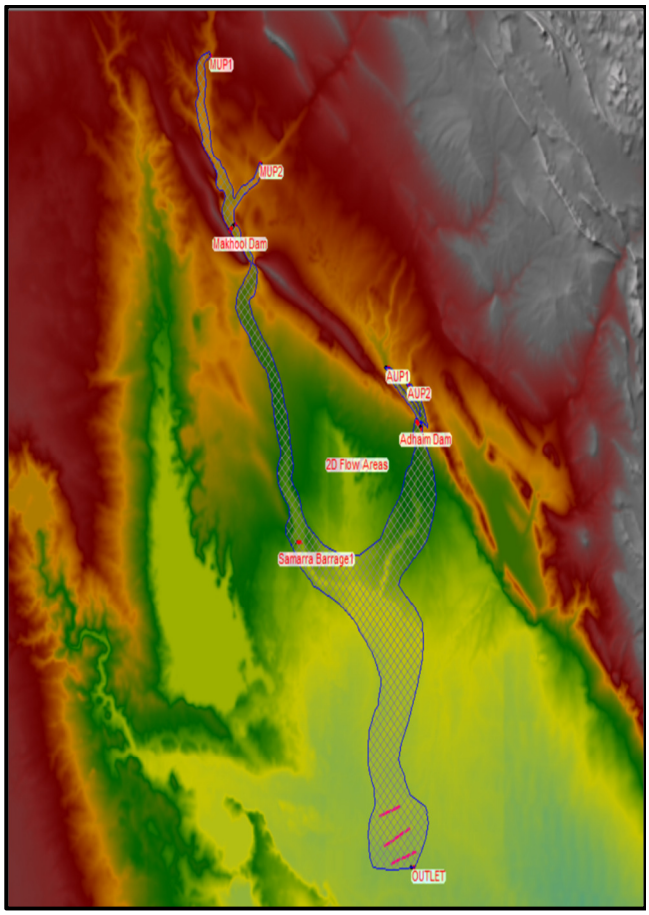


Fig. 4. TIN of the study area.

In flood or dam failure hazard simulations, the initial step is to establish the water distribution across the study area. This is achieved using boundary conditions, such as terrain elevation, reservoir levels of the Adhaim and Makhool dams, and the water depth of the Tigris River. The reservoir inflow hydrographs account for the PMF and lateral inflows from the Greater Zab and Lesser Zab rivers. The average climatic conditions during the study period were characterized by temperatures of 23.46°C and rainfall of 241.06 mm. Figure 5 displays the area-elevation and storage curves for Adhaim Dam, with elevations from 102 m to 146.5 m, based on data from [48]. For Makhool Dam, the elevation-storage curve runs from 125 m to 152.5 m, as depicted in Figure 6. These parameters were incorporated into the 2D HEC-RAS model [29].

Manning's roughness coefficient is influenced by several factors, including the grain size distribution of the bed material, channel and floodplain geometry, vegetation cover, and flow variability. It is a key parameter affecting the surface water distribution and flow dynamics. In this study, classified satellite imagery was calibrated using LC data from imported USGS NLCD (2014) polygons. Manning's n values were assigned according to the LC classes specified in the HEC-RAS Hydraulic Reference Manual. The resulting map was exported to RAS Mapper to spatially assign roughness coefficients for each categorized zone [55]. The 2D flow area utilizes a TIN-based grid, which is suitable for analysis but can lead to stability issues and longer computation times. To mitigate this, the grid size and time step are optimized based on the Courant number (Cr). Past research shows little change in the water surface elevation across various grid resolutions. Typically, a 100 m × 100 m grid is effective for modeling the flood inundation over broad, flat floodplains.

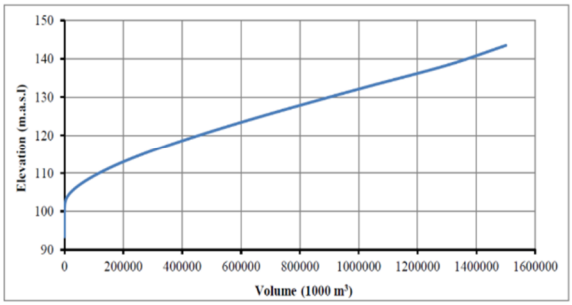


Fig. 5. Elevation -volume curves of Adhaim dam.

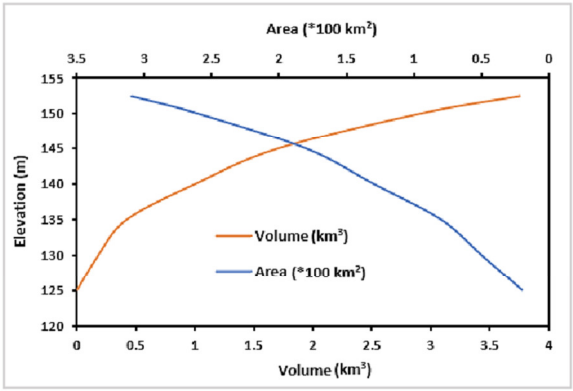


Fig. 6. Elevation -volume curves of the Makhool dam.

The total roughness of a mobile bed river includes grain-related and bed form roughness, both of which change with the flow conditions. HEC-RAS Version 6.6 addresses this by letting Manning's n vary with flow via roughness factor curves. In 2D simulations, flows are calculated as outflows from Calibration Region polygons instead of cross-sections. These regions, created in the Geometric Data Editor or RAS Mapper, can override Manning's n or set flow-dependent roughness factors. These factors depend on the outflow from each Calibration region, which might differ from the actual channel flow because of the polygon shape. To lessen the discrepancies, Calibration regions should cover the entire channel width along its length and reduce the transverse flow effects.

The study assumes an instantaneous dam failure caused by the rapid collapse of the dam's weakest section, which was the former Tigris River channel before dam construction. Routing models were created using elevation-discharge relationships, including the PMF, lateral inflows from the Greater Zab and Lesser Zab rivers, and reservoir storage-height relationships as upstream boundary conditions. A normal depth calculated with

a mean friction slope of 0.045 was used as the downstream boundary condition [56].

The HEC-RAS model utilized hydraulic structure dimensions, including the lateral slope, crest width, and dam height. A dam coefficient of 2.6 was applied for overflow scenarios, along with a discharge coefficient of 0.7. The breach shape in overflow conditions was assumed to have a lateral slope of 1:1 (height to width ratio). The two-dimensional HEC-RAS model incorporated various empirical methods to estimate the average breach width, side slope, and breach formation time. Among these, the Froehlich (2008) method was identified as the most suitable, aligning with Mosul Dam, which has similar characteristics to the Adhaim and Makhool Dams. Froehlich's approach proposes a breach side slope of 1:1 for overtopping failures [57]. Seepage through earth dams produces seepage forces, pore water pressure, and hydraulic gradients. If these factors surpass the safe limits, they can cause issues, such as piping, sloughing, or sliding, potentially leading to dam failure [58].

The primary goal of this study was to investigate the processes that lead to embankment breaches resulting from overtopping. The study highlights that while sensitive dependence on initial conditions can increase the system unpredictability, it is not necessary for such behavior to occur.

## IV. CONCLUSION

This study performed a detailed simulation of the hypothetical failure of the Al Adhaim and Al Makhool Dams to evaluate the potential downstream effects of multiple dam failures, whether happening sequentially or at the same time. Using advanced hydrodynamic modeling tools, including a two-dimensional HEC-RAS model, the research examined the flood wave movement, flood coverage, and the risks to communities, infrastructure, and the environment. The key findings of the study include:

- Investigating various dam break scenarios, focusing on the hypothetical failure of the Adhaim and Makhool Dams.
- Highlighting the cascading effects of dam failures on downstream flooding, infrastructure, ecosystems, and human communities.
- Hydrodynamic simulations are essential tools for forecasting the disaster development and impact.
- Providing insights into flood inundation extents, peak discharge rates, and available time for emergency response.
- Highlighting the importance of strong dam safety protocols, emergency response plans, and early alert systems.
- Continuing research to enhance the accuracy and reliability of the dam failure models.
- Findings inform decision-making and enhance the resilience to dam-related catastrophes.
- Encouraging stakeholders to focus on risk assessment, resource allocation, and regional strategies collaboration.
- Differentiating from previous studies by modeling multiple dam failures using a 2D HEC-RAS numerical method model.
- Focusing on overtopping and piping failures, identifying sites.
- Assessment of flood hazard and improved analysis using 2D method mapping.

Although the study provides valuable insights, it also highlights areas for future research. Possible directions include assessing the sediment transport and deposition after dam failures and creating practical guidelines for flood risk mitigation and management. These efforts would further enhance safety, preparedness, and resilience in areas vulnerable to dam-related disasters.

## ACKNOWLEDGMENT

Acknowledgment and gratitude are extended to the National Center for Studies at the Iraqi Ministry of Water Resources for their support of this research.

## REFERENCES

[1] M. Kiwanuka *et al.*, "Dam breach analysis of Kibimba Dam in Uganda using HEC-RAS and HEC-GeoRAS," *Environmental Systems Research*, vol. 12, no. 1, Oct. 2023, Art. no. 31, https://doi.org/10.1186/s40068-023-00317-4.

[2] O. Shumilova *et al.*, "Environmental effects of the Kakhovka Dam destruction by warfare in Ukraine," *Science*, vol. 387, no. 6739, pp. 1181–1186, Mar. 2025, https://doi.org/10.1126/science.adn8655.

[3] A. Annunziato *et al.*, "Modelling and Validation of the Derna Dam Break Event, " *GeoHazards*, vol. 5, no. 2, pp. 504–529, Jun. 2024, https://doi.org/10.3390/geohazards5020026.

[4] M. S. Badawy, S. A. Saleh, and M. R. Abbood, "Suggested Scenarios of Initial Filling for the Badush Reservoir, Iraq," *Tikrit Journal of Engineering Sciences*, vol. 30, no. 4, pp. 134–144, Dec. 2023, https://doi.org/10.25130/tjes.30.4.14.

[5] I. R. Karim, Z. F. Hassan, H. H. Abdullah, and I. A. Alwan, "2D-HEC-RAS Modeling of Flood Wave Propagation in a Semi-Arid Area Due to Dam Overtopping Failure," *Civil Engineering Journal*, vol. 7, no. 9, pp. 1501–1514, Sep. 2021, https://doi.org/10.28991/cej-2021-03091739.

[6] W. A. Abdulrasul and W. S. Mohammed-Ali, "Experimental Study of Energy Dissipation in Sudden Contraction of Open Channels," *Instrumentation Mesure Métrologie*, vol. 23, no. 1, Feb. 2024, https://doi.org/10.18280/i2m.230105.

[7] M. Beza, A. Fikre, and A. Moshe, "Dam Breach Modeling and Downstream Flood Inundation Mapping Using HEC-RAS Model on the Proposed Gumara Dam, Ethiopia," *Advances in Civil Engineering*, vol. 2023, no. 1, Jan. 2023, Accessed: Jul. 03, 2025, Art. no. 8864328, https://onlinelibrary.wiley.com/doi/abs/10.1155/2023/8864328.

[8] S. Solava and N. Delatte, "Lessons from the Failure of the Teton Dam," in *Third ASCE Forensic Engineering Congress*, San Diego, California, USA, Sep. 2003, pp. 178–189.

[9] F. Alcrudo and J. Mulet, "Description of the Tous Dam break case study (Spain)," *Journal of Hydraulic Research*, vol. 45, no. sup1, pp. 45–57, Dec. 2007, https://doi.org/10.1080/00221686.2007.9521832.

[10] "Association of State Dam Safety Officials (ASDSO) 2023 Dam Safety Conference," *WEST Consultants, Inc.* https://www.westconsultants.com/event/association-of-state-dam-safety-officials-asdso-2023-dam-safety-conference/.

[11] A. O. Turkel, H. Zaifoglu, and A. M. Yanmaz, "Probabilistic modeling of dam failure scenarios: a case study of Kanlikoy Dam in Cyprus," *Natural Hazards*, vol. 120, no. 11, pp. 10087–10117, Sep. 2024, https://doi.org/10.1007/s11069-024-06599-w.

[12] W. Mohammed-Ali, C. Mendoza, and R. R. Holmes, "Riverbank stability assessment during hydro-peak flow events: the lower Osage River case (Missouri, USA)," *International Journal of River Basin Management*, vol. 19, no. 3, pp. 335–343, Jul. 2021, https://doi.org/10.1080/15715124.2020.1738446.

[13] A. Del Gaudio *et al.*, "Modelling the impact of a dam-break wave on a vertical wall," *Earth Surface Processes and Landforms*, vol. 49, no. 7, pp. 2080–2095, 2024, https://doi.org/10.1002/esp.5817.

[14] A. Raman and F. Liu, "An investigation of the Brumadinho Dam Break with HEC RAS simulation." arXiv, Nov. 13, 2019, https://doi.org/10.48550/arXiv.1911.05219.

[15] A. Del Gaudio, G. Constantinescu, C. Di Cristo, F. De Paola, and A. Vacca, "Large eddy simulation of power-law fluid dam break wave impacting against a vertical wall," *Physical Review Fluids*, vol. 9, no. 7, Jul. 2024, Art. no. 074801, https://doi.org/10.1103/PhysRevFluids.9.074801.

[16] M. F. Shahrim and F. C. Ros, "Dam Break Analysis of Temenggor Dam Using HEC-RAS," *IOP Conference Series: Earth and Environmental Science*, vol. 479, no. 1, Mar. 2020, Art. no. 012041, https://doi.org/10.1088/1755-1315/479/1/012041.

[17] A. A. Khanoosh, E. H. Khaleel, and W. S. Mohammed-Ali, "The Resilience of Numerical Applications to Design Drinking Water Networks," *International Journal of Design & Nature and Ecodynamics*, vol. 18, no. 5, pp. 1069–1075, Oct. 2023, https://doi.org/10.18280/ijdne.180507.

[18] M. Ramola, P. C. Nayak, B. Venkatesh, and T. Thomas, "Dam break analysis using hec-ras and flood inundation modelling for Pulichinatala Dam in Andhra Pradesh, India," *Indian Journal of Ecology*, vol. 48, no. 2, pp. 620-626, 2021.

[19] M. Pilotti, L. Milanesi, V. Bacchi, M. Tomirotti, and A. Maranzoni, "Dam-Break Wave Propagation in Alpine Valley with HEC-RAS 2D: Experimental Cancano Test Case," *Journal of Hydraulic Engineering*, vol. 146, no. 6, Jun. 2020, Art. no. 05020003, https://doi.org/10.1061/(ASCE)HY.1943-7900.0001779.

[20] M. B. Ansori, A. A. N. S. Damarnegara, N. F. Margini, and D. A. D. Nusantara, "Flood inundation and Dam break analysis for disaster risk mitigation (a case study of way apu dam)," *GEOMATE Journal*, vol. 21, no. 84, pp. 85–92, Nov. 2021, https://geomatejournal.com/geomate/article/view/121.

[21] W. S. Mohammed-Ali and R. S. Khairallah, "Flood Risk Analysis: The Case of Tigris River (Tikrit /Iraq)," *Tikrit Journal of Engineering Sciences*, vol. 30, no. 1, pp. 112–118, Mar. 2023, https://doi.org/10.25130/tjes.30.1.11.

[22] M. Sumira, E. Anggraheni, and R. M. S. Prastica, "Dam Break Analysis of Sermo Dam," *Journal of the Civil Engineering Forum*, pp. 127–138, May 2023, https://doi.org/10.22146/jcef.5619.

[23] M. M. Altawash and H. A. Al Thamiry, "Velocity Patterns inside the Proposed Makhool Dam Reservoir with Different Operation Plans," *IOP Conference Series: Earth and Environmental Science*, vol. 1120, no. 1, Sep. 2022, Art. no. 012015, https://doi.org/10.1088/1755-1315/1120/1/012015.

[24] M. I. Huseiny, A. A. Kuntoro, E. O. Nugroho, and M. S. B. Kusuma, "Dam-Break Risk Analysis and Mitigation at Pidekso Dam, Wonogiri Regency, Central Java, Indonesia," *Journal of Water Management Modeling*, vol. 32, Aug. 2024, Art. no. C521, https://doi.org/10.14796/JWMM.C521.

[25] N. M. Al-Nedawi, S. S. Sammen, and A. Fakhri, "Modeling of Flood Wave Propagation Due to Hemren Dam Failure," *Diyala Journal of Engineering Sciences*, vol. 17, no. 3, pp. 130–145, Sep. 2024, https://doi.org/10.24237/djes.2024.17309.

[26] M. S. Badowi, S. A. Saleh, and M. R. Abbood, "Dam Breakdown and Response of Protection Dam, Case Scenarios of Mosul-Badush Dams, Northern Iraq," *Tikrit Journal of Engineering Sciences*, vol. 31, no. 1, pp. 75–87, Feb. 2024, https://doi.org/10.25130/tjes.31.1.7.

[27] L. Abdelghani, "Modeling of dam-break flood wave propagation using HEC-RAS 2D and GIS: case study of Taksebt dam in Algeria," *World Journal of Engineering*, vol. 21, no. 2, pp. 376–385, Jan. 2023, https://doi.org/10.1108/WJE-10-2022-0405.

[28] Y. Paşa, İ. B. Peker, A. Hacı, and S. Gülbaz, "Dam failure analysis and flood disaster simulation under various scenarios," *Water Science and Technology*, vol. 87, no. 5, pp. 1214–1231, Feb. 2023, https://doi.org/10.2166/wst.2023.052.

[29] M. J. Mohamed, I. R. Karim, M. Y. Fattah, and N. Al-Ansari, "Modelling Flood Wave Propagation as a Result of Dam Piping Failure Using 2D-HEC-RAS," *Civil Engineering Journal*, vol. 9, no. 10, pp. 2503–2515, Oct. 2023, https://doi.org/10.28991/CEJ-2023-09-10-010.

[30] F. T. Gebremariam, A. H. Tesfay, F. G. Sigtryggsdóttir, H. Goitom, and L. Lia, "Overtopping-Induced Embankment Breaching Experiments: State-of-the-Art Review on Measurement and Instrumentation," *Water*, vol. 17, no. 7, Apr. 2025, Art. no. 1051, https://doi.org/10.3390/w17071051.

[31] A. R. Refaiy, N. M. AboulAtta, M. A. Gad, and D. A. El-Molla, "Modeling the successive failure of complex dams systems: A necessity in the light of climatic shifts in extreme storms," *Ain Shams Engineering Journal*, vol. 15, no. 11, Nov. 2024, Art. no. 103033, https://doi.org/10.1016/j.asej.2024.103033.

[32] D. C. Froehlich, "Embankment Dam Breach Parameters and Their Uncertainties," *Journal of Hydraulic Engineering*, vol. 134, no. 12, pp. 1708–1721, Dec. 2008, https://doi.org/10.1061/(ASCE)0733-9429(2008)134:12(1708).

[33] T. C. MacDonald and J. Langridge-Monopolis, "Breaching Charateristics of Dam Failures," *Journal of Hydraulic Engineering*, vol. 110, no. 5, pp. 567–586, May 1984, https://doi.org/10.1061/(ASCE)0733-9429(1984)110:5(567).

[34] J. L. Von Thun and D. R. Gillette, "Guidance on breach parameters," *Internal Memorandum, U.S. Dept. of the Interior*, Bureau of Reclamation, Denver, CO, 1990.

[35] T. L. Wahl, "Prediction of embankment dam breach parameters—A literature review and needs assessment." *Dam Safety Rep. No.* DSO-98-004, U.S. Dept. of the Interior, Bureau of Reclamation, Denver, 1998.

[36] T. L. Wahl, "Uncertainty of Predictions of Embankment Dam Breach Parameters," *Journal of Hydraulic Engineering*, vol. 130, no. 5, pp. 389–397, May 2004, https://doi.org/10.1061/(ASCE)0733-9429(2004)130:5(389).

[37] Y. Xu and L. M. Zhang, "Breaching Parameters for Earth and Rockfill Dams," *Journal of Geotechnical and Geoenvironmental Engineering*, vol. 135, no. 12, pp. 1957–1970, Dec. 2009, doi: 10.1061/(ASCE)GT.1943-5606.0000162.

[38] J. Zhang, G. Fan, H. Li, J. Zhou, and X. Yang, "Large-scale field model tests of landslide dam breaching," *Engineering Geology*, vol. 293, Nov. 2021, Art. no. 106322, https://doi.org/10.1016/j.enggeo.2021.106322.

[39] G. Brunner, "HEC-RAS 2D User's Manual," Oct. 2024, Version 6.6.

[40] T. A. Basheer, A. Wayayok, B. Yusuf, and R. Kamal, "Dam Breach parameters and their influence on flood hydrographs for Mosul Dam," *Journal of Engineering Science and Technology*, vol. 12, no. 11, pp. 2896-2908, Nov. 2017.

[41] C. Kaya, "Multi-failure analysis of Seyhan dam and Çatalan dam," M.S. thesis, Fen Bilimleri Enstitüsü, Istanbul, Turkey, 2018.

[42] W. Mohammed-Ali, "Minimizing the detrimental effects of hydro-peaking on riverbank instability: The lower Osage River case, " Ph.D. dissertation, University of Science and Technology, Missouri, USA, Jan. 2020.

[43] R. González Blanch, "Effect of the sub-grid geometry on two-dimensional river flow models," Bachelor thesis, Universitat Politècnica de Catalunya, Barcelona, Spain, 2017.

[44] A. Jha, "Object-oriented hyperbolic solver on 2D-unstructured meshes applied to the shallow water equations," Ph.D. dissertation, Department of Civil and Building Engineering, Loughborough University, Loughborough, UK, 2006.

[45] H. H. Hussain *et al.*, "Modifying the spillway of Adhaim Dam, reducing flood impact, and saving water," *Journal of Water Management Modeling*, vol. 30, Apr. 2022, Art. no. C485, https://doi.org/10.14796/JWMM.C485.

[46] N. J. Rasheed, M. S. Al-Khafaji, and I. A. Alwan, "Assessing the influence of climate change on sediment dynamics in the proposed makhool dam reservoir, Iraq," *Engineering and Technology Journal*, vol.

42, no. 5, pp. 604–614, Apr. 2024, https://doi.org/10.30684/etj.2024.146620.1690.

[47] A. M. Hadi *et al.*, "GIS-Based Rainfall Analysis using Remotely Sensed Data in Kirkuk Province, Iraq: Rainfall Analysis," *Tikrit Journal of Engineering Sciences*, vol. 29, no. 4, pp. 48–55, Dec. 2022, https://doi.org/10.25130/tjes.29.4.6.

[48] "World Bank Climate Change Knowledge Portal." https://climateknowledgeportal.worldbank.org/.

[49] T. S. Khayyun, "Mathematical Modeling of Hypothetical Failure of Multiple Dams-Mosul and Makhool Dams as a Case Study", Ph.D. dissertation, Department of Building and Construction Engineering, University of Technology, Baghdad, Iraq, 2006.

[50] N. Al-Ansari, N. Adamo, V. K. Sissakian, S. Knutsson, and J. Laue, "Water Resources of the Tigris River Catchment," *Journal of Earth Sciences and Geotechnical Engineering*, vol. 8, no. 3, pp. 21-42, 2018.

[51] K. M. Mahmood and W. S. Mohammed-Ali, "A Hydraulic Performance Model of Khassa Chai River under Varying Flow Conditions," *Engineering, Technology & Applied Science Research*, vol. 15, no. 2, pp. 20934–20940, Apr. 2025, https://doi.org/10.48084/etasr.9675.

[52] O. T. N. Al-Tikrity, R. H. Irzooki, and S. A. Saleh, "Hydrological and Geometric Analysis of a Proposed Reservoir on the Upper Zab River Using GIS and Remote Sensing Techniques," *Tikrit Journal of Engineering Sciences*, vol. 32, no. 1, pp. 1–12, Feb. 2025, https://doi.org/10.25130/tjes.32.1.1.

[53] T. Hein *et al.*, "Current status and restoration options for floodplains along the Danube River," *Science of The Total Environment*, vol. 543, pp. 778–790, Feb. 2016, https://doi.org/10.1016/j.scitotenv.2015.09.073.

[54] W. A. Abdulrasul and W. S. Mohammed-Ali, "Experimental Study of Energy Dissipation in Sudden Contraction of Open Channels," *Instrumentation Mesure Métrologie*, vol. 23, no. 1, pp. 55-61, Feb. 2024, https://doi.org/10.18280/i2m.230105.

[55] "EarthExplorer." https://earthexplorer.usgs.gov/.

[56] A. S. Al-Fahal, A. S. Ahmed, A. K. Mohammed, and W. S. Mohammed-Ali, "Evaluation of Rainwater Harvesting Systems for Drinking Water Quality in Iraq," *International Journal of Design & Nature and Ecodynamics*, vol. 19, no. 1, pp. 111–117, Feb. 2024, https://doi.org/10.18280/ijdne.190113.

[57] I. I. Ghdhban and R. H. Irzooki, "Estimating the Sediment Load Transported by the Valleys to Makhoul Dam Reservoir (Under Construction)," *Tikrit Journal of Engineering Sciences*, vol. 31, no. 2, pp. 255–271, Jun. 2024, https://doi.org/10.25130/tjes.31.2.24.

[58] A. A. J. Jamel and H. F. Hassan, "Effect of Core Angle in Earth Dam on Seepage Characteristic (Numerical Model)," *Tikrit Journal of Engineering Sciences*, vol. 32, no. 1, pp. 1–10, Mar. 2025, https://doi.org/10.25130/tjes.32.1.26.